Supplementary information

Unprecedented trinuclear Fe(II) triazole-based complex exhibiting a concerted and complete sharp spin transition above room temperature

Narsimhulu Pittala,[a] Franck Thétiot,[a] Smail Triki,*[a] Kamel Boukheddaden,[b] Guillaume Chastanet[c] and Mathieu Marchivie.[c]

[a]UMR CNRS 6521, Chimie, Electrochimie Moléculaires, Chimie Analytique, Université de Bretagne Occidentale, C.S. 93837 - 29238 Brest Cedex 3 –France
*e-mail : smail.triki@univ-brest.fr
[b] Groupe d'Etudes de la Matière Condensée, UMR-CNRS 8635, Université de Versailles (Paris-Saclay), 45 Avenue des Etats-Unis 78035 Versailles, France.
[c]CNRS, Université Bordeaux, ICMCB, 87 Av. Doc. A. Schweitzer, F-33608 Pessac, France.

1 - Trinuclear Fe(II) Complexes Based on Functionalized 4-R-1,2,4-Triazole Ligands

Table S1. Trinuclear Fe_3 complexes with triple triazole bridges

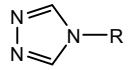 **(trz-R)**	**Trinuclear complex**	**SCO behavior / $T_{1/2}$**	**Ref**
trz—CH_2-CH_2-CH_3	$[Fe_3(Prtrz)_6(ReO_4)_4(H_2O)_2](ReO_4)_2 \cdot H_2O$	gradual / $T_{1/2}$=185 K	1a
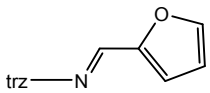	$[Fe_3(furtrz)_6(ptol)_2(MeOH)_4](ptol)_4 \cdot 4(MeOH)$	gradual / $T_{1/2}$~170 K	1b
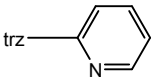	$[Fe_3(Pytrz)_8(H_2O)_4](NO_3)_6$	Gradual / $T_{1/2}$=208 K	2a
	$[Fe_3(Pytrz)_8(H_2O)_4](ClO_4)_6$	HS	2a
	$[Fe_3(Pytrz)_8(H_2O)_4](Br)_6$	HS	2a
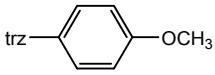	$[Fe_3(MeOptrz)_8(H_2O)_4](BF_4)_6 \cdot 2H_2O$	HS	2b
	$[Fe_3(MeOptrz)_6(H_2O)_6](Tos)_6 \cdot 4H_2O$	gradual / $T_{1/2}$=245 K	2b
	$[Fe_3(MeOptrz)_6(H_2O)_6](Tos)_6$	gradual / $T_{1/2}$=330 K	2b
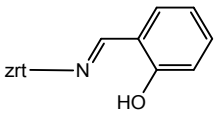	$[Fe_3(Hsaltrz)_6(H_2O)_2(EtOH)_4](ClO_4)_6 \cdot 2EtOH$	HS	3a
trz—CH_2-CH_2-OH	$[Fe_3(Hyetrz)_6(H_2O)_6](CF_3SO_3)_6$	gradual / $T_{1/2}$=290 K	3b
trz—CH_2-CH_3	$[Fe_3(Ettrz)_6(H_2O)_6](CF_3SO_3)_6$	abrupt / $T_{1/2}$=205 K	3c
trz—$CH(CH_3)_2$	$[Fe_3(iPrtrz)_6(H_2O)_6](Tos)_6 \cdot 2H_2O$	gradual / $T_{1/2}$=242 K	3d
	$[Fe_3(iPrtrz)_6(H_2O)_6](CF_3SO_3)_6$	gradual / $T_{1/2}$=185 K	3d
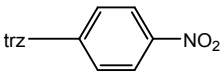	$[Fe_3(Nptrz)_6(H_2O)_2(EtOH)_4](ptol)_6 \cdot 4EtOH$	gradual / $T_{1/2}$=148 K	3e
trz—CH_2-CH_2-SO_3^-	$[Fe_3(Settrz)_6(H_2O)_6].5H_2O$	spin transition with $T_{1/2}(\uparrow)$=357 K, $T_{1/2}(\downarrow)$ =343K	4a
trz—CH_2-$CH(SO_3^-)_2$	$(Me_2NH_2)_6[Fe_3(dSettrz)_6(H_2O)_6]$	spin transition with $T_{1/2}(\uparrow)$=400 K, $T_{1/2}(\downarrow)$ =310K	4b

MeOptrz = 4-(p-methoxyphenyl)-1,2,4-triazole; Tos = p-toluenesulfonate; Hsaltrz = N-salicylidene 4-amino-1,2,4-triazole; Prtrz = 4-propyl-1,2,4-triazole; Hyetrz = 4-(2'-hydroxyethyl)-1,2,4-triazole; Ettrz = 4-ethyl-1,2,4-triazole; iPrtrz = 4-isopropyl-1,2,4-triazole; Nptrz = 4-(4'-nitrophenyl)-1,2,4-triazole); ptol = p-tolylsulfonate); Pytrz = 4-(2-pyridyl)-1,2,4-triazole; bpy = 2,2'-bipyridyl; tpen = tetrakis(2-pyridylmethyl)ethylendiamine; $HC(3,5\text{-}Mepz)_3$ = tris(3,5-dimethylpyrazol-1-yl)methane; ddb = N2,N2,N4,N4-tetrabutyl-N6,N6-di(pyridin-2-yl)-1,3,5-triazine-2,4,6-triamine; pytepy = 2-(1H-pyrazol-1-yl)-6-(1H-tetrazol-5-yl)pyridine; Settrz = 4-(1,2,4-triazol-4-yl)ethanesulfonate; dSettrz = 4-(1,2,4-triazol-4-yl)ethanedisulfonate; furtrz = 1,2,4-triazole ligand furanylidene-4H-1,2,4-triazol-4-amine.

2 - Syntheses

a - General Considerations

All the starting reagents were purchased from commercial sources (Sigma-Aldrich, Across, Fisher Scientific, Alfa Aesar and Merck) and used without further purification unless otherwise stated. Deuterated solvents were purchased from Sigma-Aldrich and Cambridge Isotope Laboratories. Dried solvents were prepared by refluxing for one day under nitrogen over the appropriate drying agents (calcium hydride for acetonitrile, dichloromethane, and hexane; magnesium and iodine for methanol; sodium for ethanol, and molecular sieves for DMF), and then degassed before use. Solvents were stored in glass ampoules under argon. All the glassware and cannula were stored in an oven (>373 K). The reactions were carried out under argon/nitrogen by using the Schlenck techniques. Thin layer chromatography (TLC) analysis was performed on pre-coated silica gel aluminium-backed plates (silica gel $60F_{254}$). The organic compounds were purified using flash column chromatography on silica gel (230-400 mesh). ^{1}H and ^{13}C-NMR spectra were recorded on Bruker-300, Bruker-400 and Bruker-500 spectrometers, and the spectra were referenced internally using residual proton solvent resonances relative to tetramethylsilane ($\delta = 0$ ppm). Infrared (IR) spectra were recorded in the range of 4000-200 cm^{-1} on a FT-IR BRUKER ATR VERTEX70 Spectrometer. Elemental analyses were performed at the "Service de microanalyse", CNRS, 91198 Gif-sur-Yvette, France.

N.B.: Because of the use of organic ligands composed with cyano functional groups, all the experiments reported here have been undergone with great caution, especially considering the eventual release of the gases HCN and related derivatives that are poisonous and potentially lethal at low levels. Consequently, all those compounds should be prepared and handled behind suitable protective shields. In this context, all the waste involving polynitrile compounds were destroyed using a specific basic bath containing a saturated ethanolic solution of KOH mixed with an aqueous solution of NaOCl, while the glassware were cleaned using a basic bath consisting of a saturated ethanol/water solution of KOH (1:1 volume ratio).

b - Syntheses of the ligands

Triazole-based Ligand. The 4-(Benzyl)-1,2,4-triazole (bntrz) ligand was synthesized using the previously reported method.[5,6]

Cyanocarbanion Salt. The potassium 1,1,3,3-tetracyano-2-thioethylpropenide (K(tcnset)) was prepared in two steps (Scheme S1). In the first step, 2-[(bis-ethylthio)methylene]malononitrile was synthesized from malononitrile and alkyl halide following the reported methods.[7a-b] Then, potassium [1,1,3,3-tetracyano-2-thioethylpropenide] salt [K(tcnset)] was obtained according to modified literature methods, from the corresponding ketene thioacetal after reaction with malononitrile in the presence of potassium tert-butoxide.[7c]

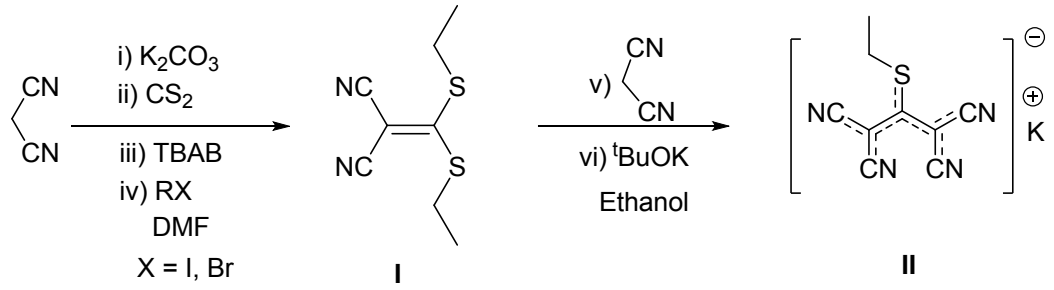

Scheme S1. Synthesis of K(tcnset).

2-[(bis-ethylthio)methylene]malononitrile (I). To a solution of malononitrile (4.0 g, 60.55 mmol) in DMF (25 mL) was added K_2CO_3 (8 g, 57.88 mmol). After stirring for 30 min at room temperature, CS_2 (3.6 mL, 66.6 mmol) was added dropwise, and the reaction mixture was stirred at room temperature for an additional 10 min before ethylhalide (121.1 mmol) and tetrabutylammonium bromide (4 g, 10 mmol) were successively added. After further stirring the for 30 minutes at room temperature, the reaction mixture was then refluxed for 2 h at 50 ^oC. Subsequently, after stirring for 24-48 h at room temperature while monitoring the reaction status with TLC (2:98 Ethylacetate: Hexane), the reaction mixture was diluted with water (200 mL) and extracted with Et_2O (4×200 mL). The combined organic layers were washed with Brine solution (100 mL) and dried over $MgSO_4$, then filtered and concentrated under reduced pressure. The crude product was purified by chromatography on silica gel [hexane/EtOAc, 10:0 to 9.5:0.5 (v/v)] to provide ketene dithioacetal as pale green solid (yield: 60 %, 7.170 g).

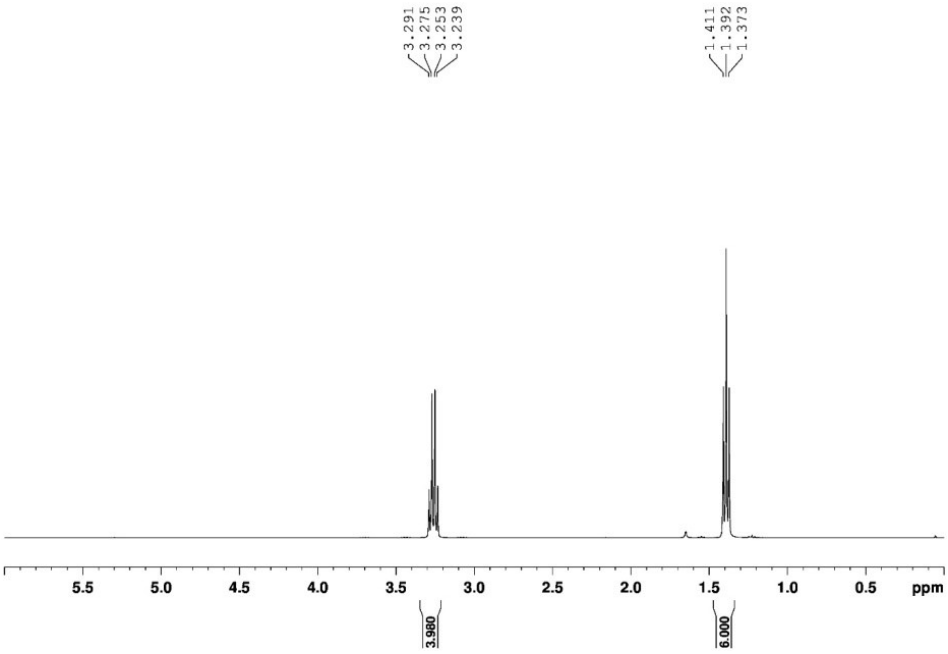

Figure S1. ^{1}H NMR (400 MHz, $CDCl_3$, 298 K) of 2-[bis(ethylthio)methylene]malononitrile (**I**). ^{1}H NMR: δ, 3.27 (q, 4H,-SCH_2-), 1.39 (t, 6H,-CH_3).

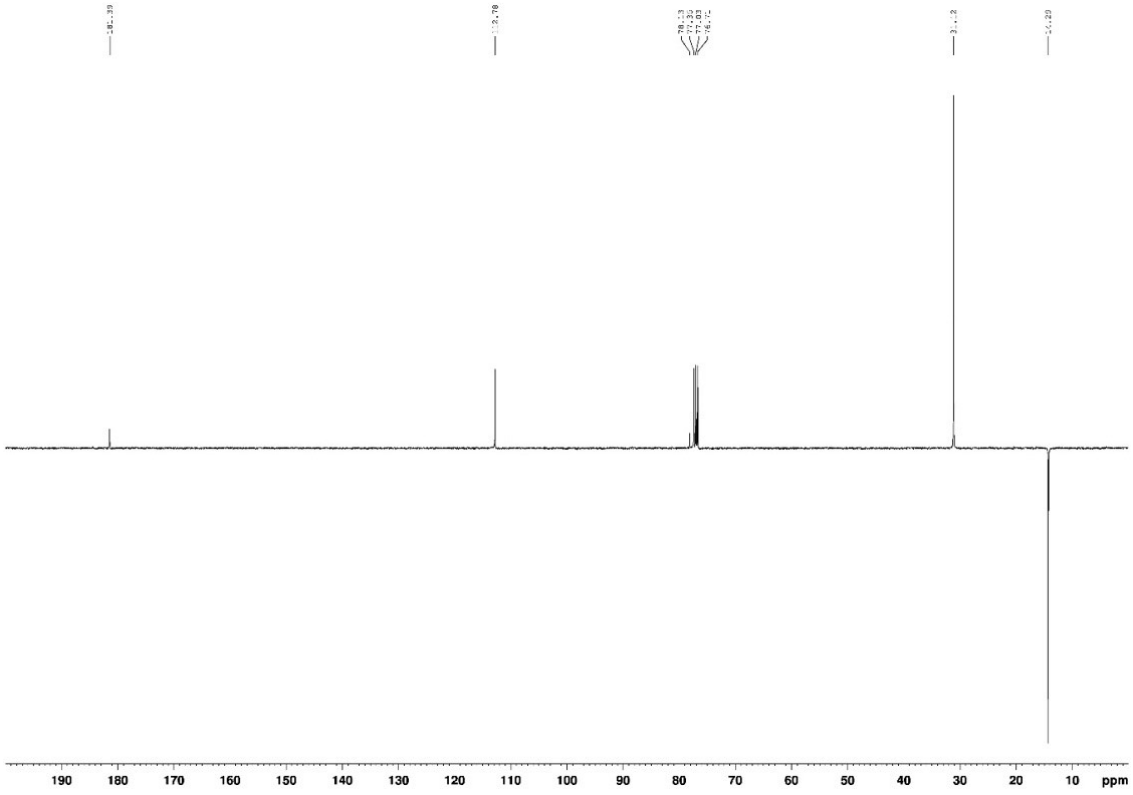

Figure S2. ^{13}C NMR (400 MHz, $CDCl_3$, 298 K) of 2-[bis(ethylthio)methylene]malononitrile (**I**). ^{13}C NMR: δ, 181.4 (-$\underline{C}$(S-Et)$_2$), 112.8 (-CN), 78.1 (-$\underline{C}$(CN)$_2$), 31.1 (-SCH_2-), 14.3 (-CH_3).

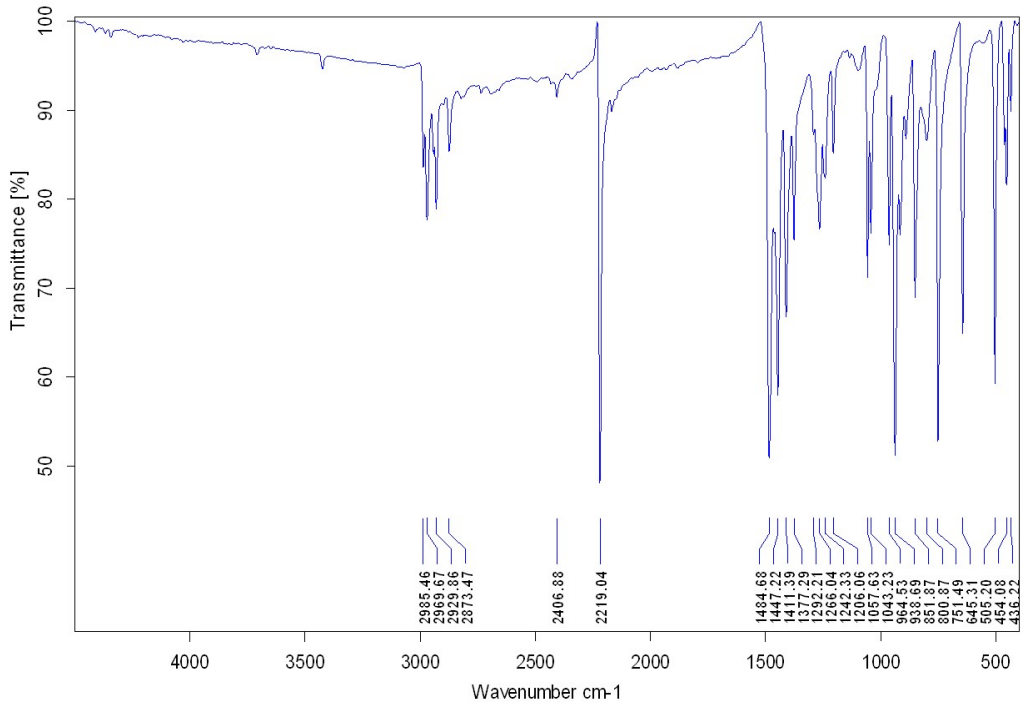

Figure S3. Infrared Spectrum of 2-[bis(ethylthio)methylene]malononitrile (**I**). IR data (ν, cm^{-1}): 2970w, 2930w, 2874w, 2407w, 2349w, 2322w, 2219s, 1486s, 1463m, 1411w, 1377w, 1265w, 1240w, 1206w, 1057m, 1043m, 964s, 939w, 852w, 801w, 751w, 646m, 505m, 454m, 436w.

K(tcnset) (II). In this second step, a warm ethanolic solution (30 mL) of the previously synthesized 2-[(bis-ethylthio)methylene]malononitrile (**I**) (1.983 g, 10 mmol) was added dropwise to an ethanolic solution (10 mL) of malononitrile (0.66 g, 10 mmol) and t-BuOK (1.12 g, 10 mmol). The resulting mixture was refluxed for 1h, and then cooled to room temperature and kept at 4°C for two days. The compound was filtered on a sintered-glass funnel, washed with distilled diethyl ether, and finally dried under vacuum to obtain the potassium salt of [1,1,3,3-tetracyano-2-thioalkylpropenide] (K(tcnset), **II**) as a white crystalline powder (yield: 86 %, 2.076 g).

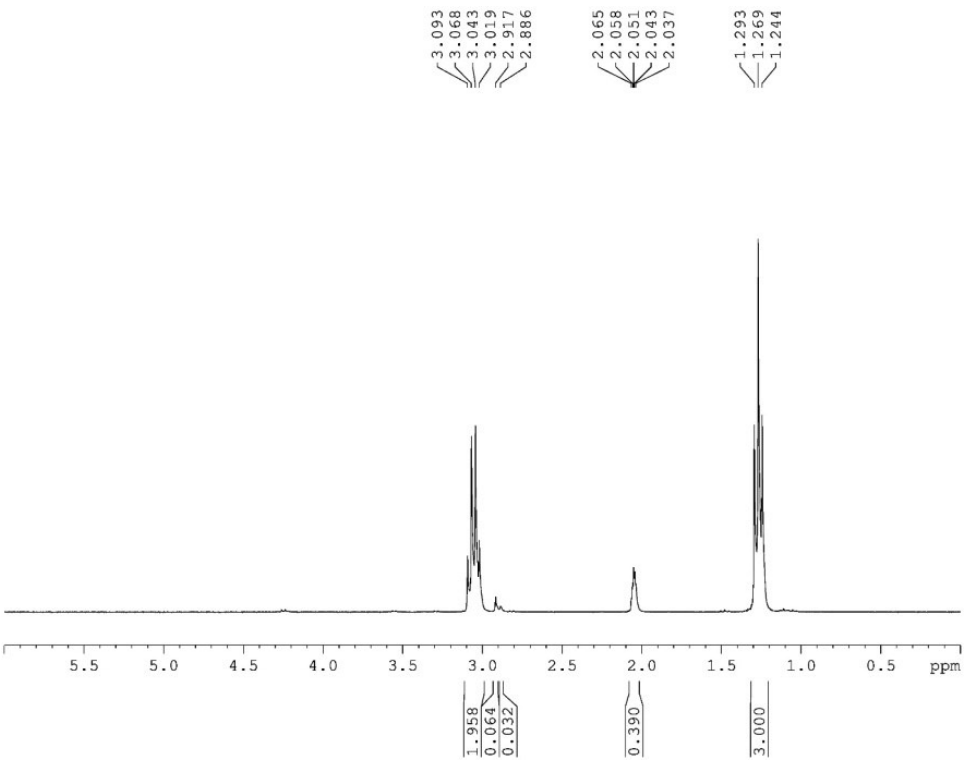

Figure S4. ^{1}H NMR (300 MHz, Acetone-D_6, 298 K) of K(tcnset) (**II**). ^{1}H NMR: δ, 3.06 (q, 2H, -SCH_2-), 1.27 (t, 3H -CH_3).

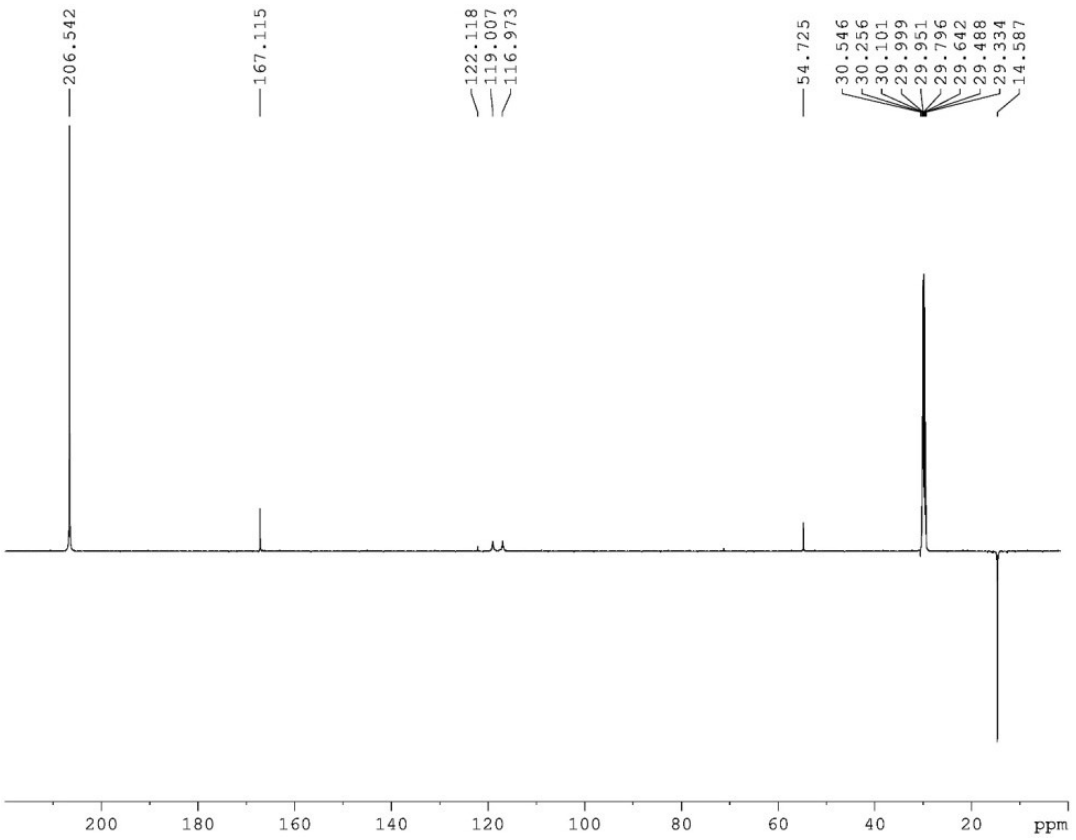

Figure S5. ^{13}C NMR (500 MHz, Acetone-D_6, 298 K) of K(tcnset) (**II**). ^{13}C NMR: δ, 167.1 (-C(S-Pr)$_2$), 119.1 (-CN), 116.9 (-CN), 54.7 (-C(CN)$_2$), 29.8 (-SCH_2-), 14.6 (-CH_3).

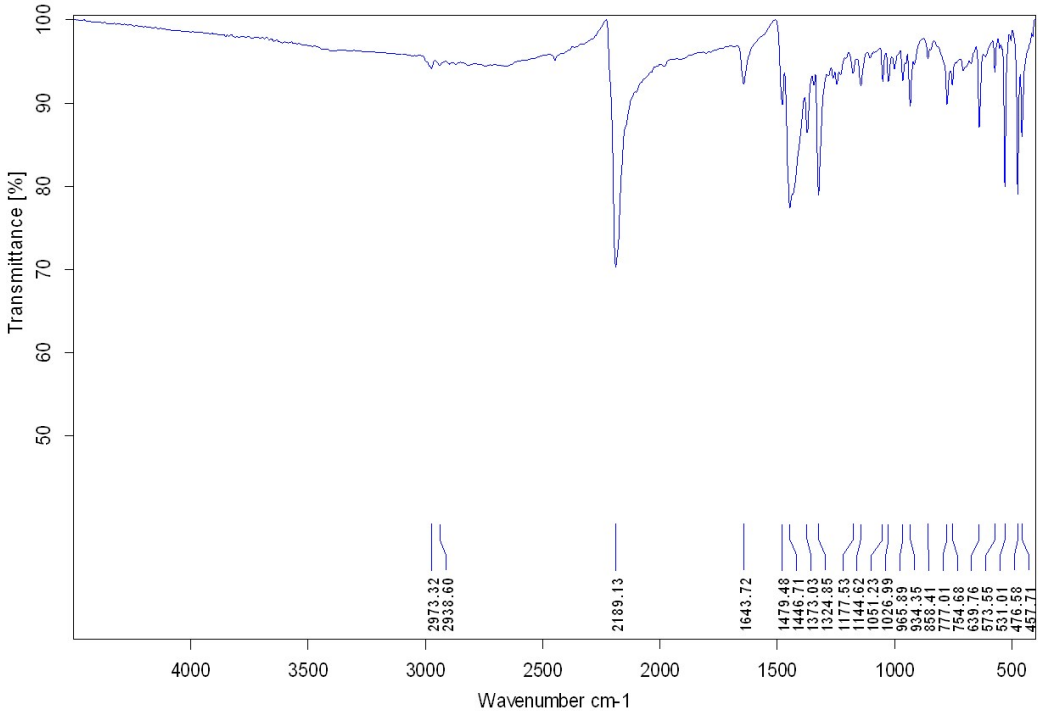

Figure S6. Infrared Spectrum of K(tcnset). IR (ν, cm^{-1})**:** 2189s, 1644w, 1445s, 1373w, 1325w, 934w, 777w, 640w, 531w, 477w, 458w.

c - Single-crystals preparation of $[Fe_3(bntrz)_6(tcnset)_6]$ (1)

Single-crystals of linear trinuclear Fe(II) SCO complex $[Fe_3(bntrz)_6(tcnset)_6]$ were prepared by slow diffusion, in a fine glass tube (3.0 mm diameter). An aqueous solution of $Fe(BF_4)_2 \cdot 6H_2O$ (33.755 mg, 0.1 mmol) and K(tcnset) (48 mg, 0.2 mmol) in 10 mL of distilled water with a small amount of ascorbic acid and a solution of bntrz (47.7 mg, 0.3 mmol) in 2.5 mL of methanol were initially prepared. The aqueous solution of Fe^{II} was placed in the bottom of a fine tube of 3.0 mm, upon which a solvent mixture of water and methanol - with a ratio of 2:1 - was carefully added. Then, a methanolic solution of bntrz of methanol was carefully layered on top of the buffer layer. Pink single crystals of **1** suitable for X-ray diffraction were grown at the interface over a period of three weeks. Alternatively, an aqueous solution of $Fe(BF_4)_2 \cdot 6H_2O$ placed at the bottom of a glass tube was covered with water mixture, over which an aqueous solution of the bntrz ligand and K(tcnset salt) was layered. The same pink single crystals of **1** were obtained in smaller size compared to the above-mentioned experimental conditions. Anal. Calcd for $C_{108}H_{84}Fe_3N_{42}S_6$: C, 55.6; H, 3.6; N, 25.2 %. Found: C, 56.1; H, 3.5; N, 24.8 %.

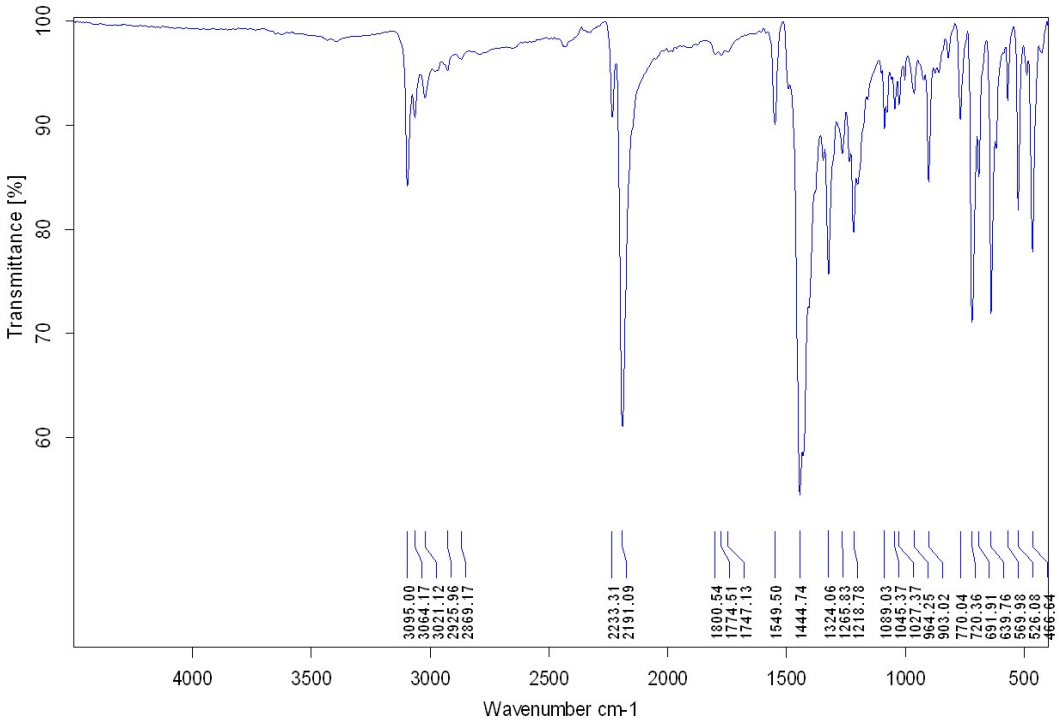

Figure S7. IR Spectrum of the Single-Crystals of $[Fe_3(bntrz)_6(tcnset)_6]$ (**1**) (4000-450 cm^{-1}). IR (ν, cm^{-1}): 3095w, 3064w, 3021w, 2233w, 2191s, 1549w, 1445s,1324s, 1219m, 1089w, 1045w, 1027w, 903w, 721m, 641m, 527w, 467w.

3 - Physical Measurements and characterizations

Single crystal X-ray studies were performed from 360 K to 250 K on Bruker-Nonius κ-CCD diffractometer using Mo Kα radiation (λ = 0.71073 Å). The corresponding structures were solved by direct methods with the SHELXS program and refined on F^2 by weighted full matrix least-squares methods using the SHELXL program.[8] All non-hydrogen atoms were refined anisotropically, hydrogen atoms were located in difference Fourier maps, and treated using a riding model. At 250 K crystal refinement was performed using an extra parameter corresponding to the proportion of the two components of a twin. The two components were related by the following twin matrix: 010 100 00-1. The two components ratio was refined to 0.82/0.18. Crystallographic data and refinement details are provided in Table S2. Magnetic measurements were performed with a Quantum Design MPMS-XL-5 SQUID magnetometer, in settle mode between 2-300 K, with an applied magnetic field of 2 Tesla, and scan rate of 0.7 $K•min^{-1}$ on single crystals of compound **1** (mass of 6.7 mg). Irradiation of **1** was carried out at 10 K with a power of 6 $mW.cm^{-2}$ at 510 nm. DSC measurements were performed on a DSC-1/LN2 Mettler Toledo calorimeter setting the heat flow scan rate at s = 2 $K•min^{-1}$ on single crystals of **1** (mass of 4.40 mg).

4 - X-ray crystallography

Table S2. Crystal data and structural refinement parameters for compound **1.**

Compound	**$[Fe_3(bntrz)_6(tcnset)_6]$ (1)**	
Temperature / K	360(2)	250(2)
Color	Yellow	Pink
Empirical formula	$C_{108}H_{84}Fe_3N_{42}S_6$	$C_{108}H_{84}Fe_3N_{42}S_6$
Formula weight /g.mol^{-1}	2330.08	2330.08
Wavelength / Å	0.71073 Å	0.71073 Å
Crystal system	Trigonal	Trigonal
Space group	$R\bar{3}$	$R\bar{3}$
a / Å	26.055(3)	25.3984(13)
c / Å	14.8240(13)	14.7341(13)
Volume / Å^3	8715(2)	8231(1)
Z	3	3
D_{calc} / g.cm^{-3}	1.332	1.410
Abs. coef. / cm^{-1}	5.43	5.75
F(000)	3600.0	3600.0
Crystal size / mm^3	0.25 × 0.02 × 0.02	0.25 × 0.06 × 0.06
2θ range / °	5.51 to 50.738	6.416 to 54.994
Refl. collected	24948	102008
Unique refl. / Rint	3544 / 0.0922	4188 / 0.0731
Data / restr. / N_v	2092 / 0 / 241	3574 / 0 / 242
Final R indexes [I>=2σ (I)]	R_1 = 0.0554, wR_2 = 0.0954	R_1 = 0.0336, wR_2 = 0.0821
Final R indexes [all data]	R_1 = 0.1214, wR_2 = 0.1125	R_1 = 0.0455, wR_2 = 0.0853
[c]GooF	1.006	1.039
$\Delta\rho_{max/\ min}$ / eÅ^{-3}	+0.341 / -0.381	+0.406/ -0.291
CCDC No.	1500725	1547824
Variable temperature structural investigations (280-345 K). The crystal structure of **1** has been solved every 5 K around the transition region, *i.e.* between 280 K and 345 K (see CCDC numbers 1500728-1500740, ESI†). The data have been recorded with a short exposure time just to follow the evolution of some key parameters as cell parameter and Fe-N bond lengths consequently they show a relatively low Observed / Unique reflections ratio. This low ratio induces some imperfections of the refined crystal structures that lead to a few B alerts in the checkcif, that concern especially the slightly distorted Ethyl branch of the Anion.		

[a]R1 = $\sum|F_o-F_c|/F_o$. [b]wR2= $\{\sum[w(F_o^2-F_c^2)^2]/\sum[w(F_o^2)^2]\}^{1/2}$. [c]GooF= $\{\sum[w(F_o^2-F_c^2)^2]/(N_{obs}-N_{var})\}^{1/2}$

Table S3. Fe-N bond lengths and N-Fe-N bond angles at 360 and 250 K for **1.**

T / K	**360 (*HS* State)**	**250 (*LS* State)**
Fe1-N1$^{(b)}$	2.175(2)	1.9785(14)
Fe1-N1$^{(a)}$	2.175(2)	1.9785(14)
Fe1-N1$^{(d)}$	2.175(2)	1.9786(14)
Fe1-N1$^{(e)}$	2.175(2)	1.9784(14)
Fe1-N1	2.175(2)	1.9785(14)
Fe1-N1$^{(c)}$	2.175(2)	1.9785(14)
Fe2-N2	2.170(2)	1.9589(15)
Fe2-N2$^{(b)}$	2.170(2)	1.9589(15)
Fe2-N2$^{(c)}$	2.170(2)	1.9589(15)
Fe2-N4$^{(c)}$	2.146(3)	1.9398(16)
Fe2-N4	2.146(3)	1.9398(16)
Fe2-N4$^{(b)}$	2.146(3)	1.9398(16)
N1$^{(b)}$-Fe1-N1$^{(d)}$	89.34(8)	90.18(5)
N1-Fe1-N1$^{(e)}$	89.34(8)	90.18(5)
N1$^{(b)}$-Fe1-N1$^{(e)}$	180.0	180.0
N1$^{(a)}$-Fe1-N1$^{(e)}$	90.67(8)	89.82(5)
N1$^{(d)}$-Fe1-N1$^{(c)}$	180.0	180.0
N1-Fe1-N1$^{(c)}$	90.66(8)	89.81(5)
N1$^{(b)}$-Fe1-N1	90.66(8)	89.82(5)
N1$^{(b)}$-Fe1-N1$^{(a)}$	89.34(8)	90.18(5)
N1$^{(d)}$Fe1-N1	89.34(8)	90.19(5)
N1$^{(b)}$-Fe1-N1$^{(c)}$	90.66(8)	89.82(5)
N1$^{(a)}$-Fe1-N1	180.0	180.0
N1$^{(d)}$-Fe1-N1$^{(a)}$	90.66(8)	89.81(5)
N1$^{(a)}$-Fe1-N1$^{(c)}$	89.34(8)	90.19(5)
N1$^{(d)}$-Fe1-N1$^{(e)}$	90.66(8)	89.82(5)
N1$^{(e)}$-Fe1-N1$^{(c)}$	89.34(8)	90.19(5)
N2-Fe2-N2$^{(c)}$	90.27(9)	90.18(6)
N2$^{(b)}$-Fe2-N2$^{(c)}$	90.28(9)	90.18(6)
N2$^{(b)}$-Fe2-N2	90.27(9)	90.18(6)
N4$^{(c)}$-Fe2-N2	177.19(9)	178.80(6)
N4-Fe2-N2	87.01(9)	88.66(6)
N4-Fe2-N2$^{(b)}$	177.19(9)	178.80(6)
N4-Fe2-N2$^{(c)}$	89.03(9)	89.52(6)
N4$^{(b)}$-Fe2-N2	89.03(9)	89.52(6)
N4$^{(b)}$-Fe2-N2$^{(c)}$	177.19(9)	178.80(6)
N4$^{(c)}$-Fe2-N2$^{(c)}$	87.01(9)	88.66(6)
N4$^{(c)}$-Fe2-N2$^{(b)}$	89.03(9)	89.52(6)
N4$^{(b)}$-Fe2-N2$^{(b)}$	87.01(9)	88.66(6)
N4$^{(c)}$-Fe2-N4	93.65(9)	91.63(6)
N4$^{(b)}$-Fe2-N4	93.65(9)	91.63(6)
N4$^{(b)}$-Fe2-N4$^{(c)}$	93.65(9)	91.63(6)

*The two Fe(II) environments are defined by N1 ([Fe1$(N1)_6$]) and by N2 and N4 ([Fe2$(N2)_3(N4)_3$]) nitrogen atoms. Symmetry transformations used to generate equivalent atoms: (a) = 2/3-x,4/3-y,1/3-z; (b) = 1-y,1+x-y,+z; (c) = +y-x,1-x,+z; (d) = 2/3-y+x,1/3+x,1/3-z; (e) = -1/3+y,1/3-x+y,1/3-z.

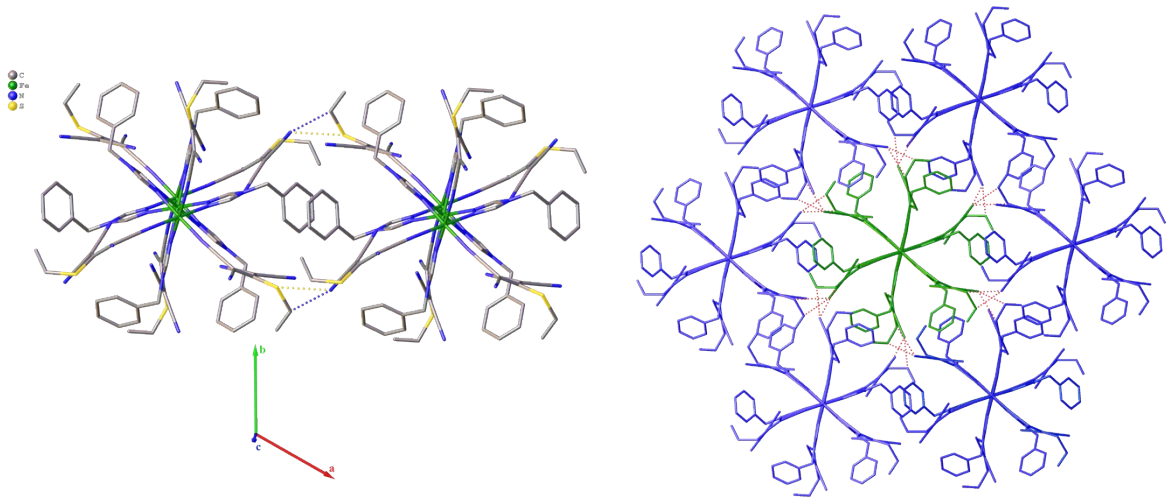

(a) (b)

Figure S8. View of the crystal structure of **1** along 'c' direction showing the van der Waals interactions between (**a**) two trinuclear systems and (**b**) between one trinuclear system and all its neighbours.

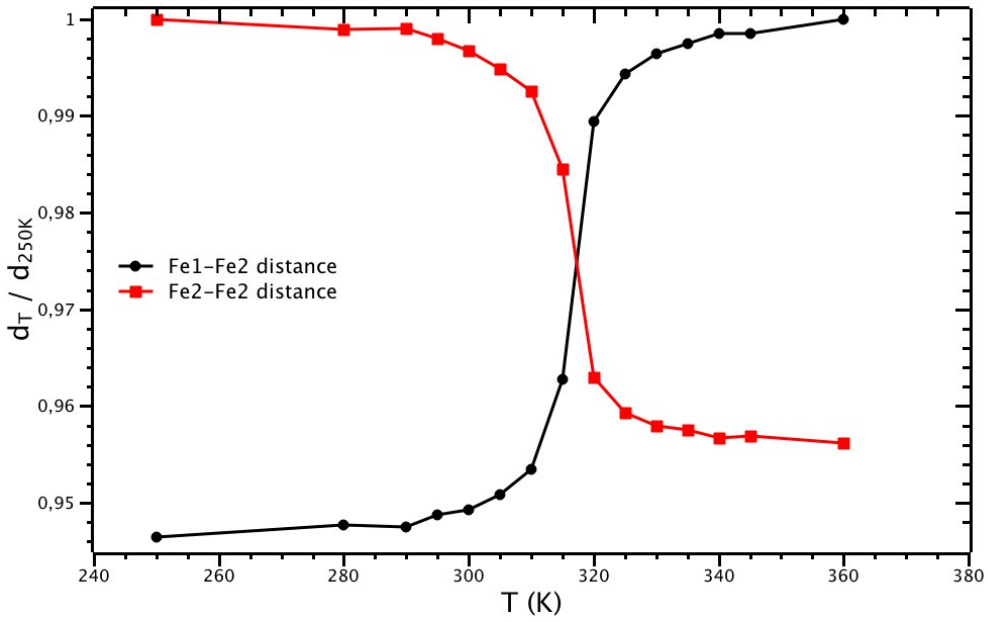

Figure S9. Evolution of the normalized distances with temperature corresponding to the intratrinuclear Fe1-Fe2 distance (black circles) and intertrinuclear Fe2···Fe2 distance along the pseudo chain axis (red square). Normalized distances are defined as d_T/d_{250K} where d_T stand for the distance at the temperature T and d_{250K} the corresponding distance at 250K. See cif files: CCDC 1500725, 1547824 and 1500728-1500740.

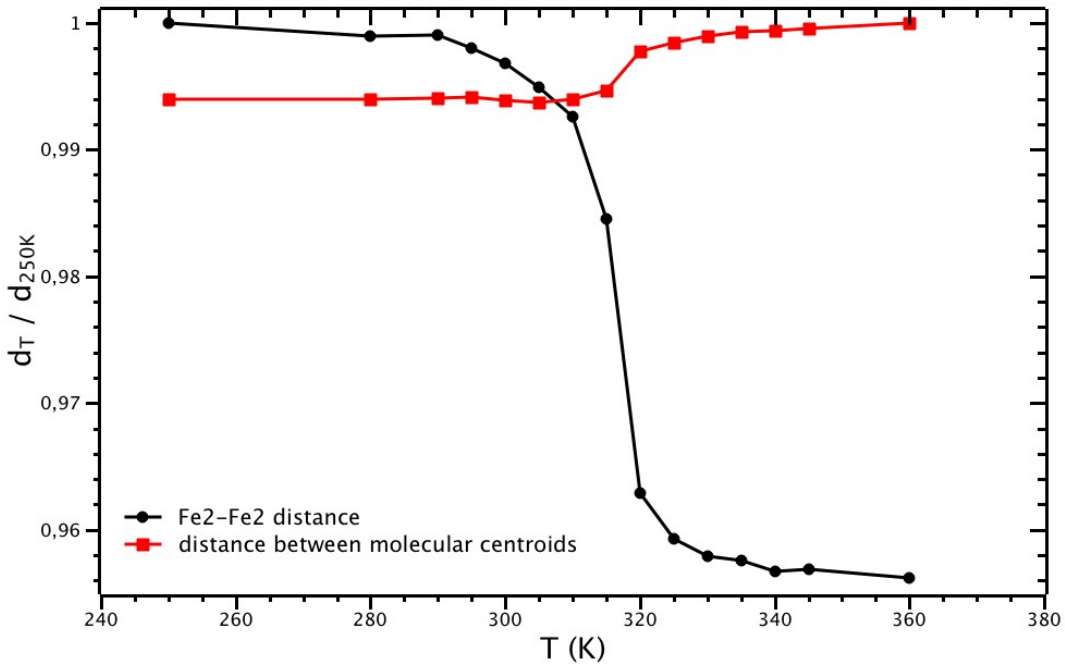

Figure S10. Evolution of the normalized distances with temperature corresponding to the intertrinuclear Fe2···Fe2 distance (black circles) and intertrinuclear distance between the molecular centroids (red square) along the pseudo chain axis. Normalized distances are defined as d_T/d_{250K} where d_T stand for the distance at the temperature T and d_{250K} the corresponding distance at 250K. See cif files: CCDC 1500725, 1547824 and 1500728-1500740.

5 - References

1. (a) M. B. Bushuev, L. G. Lavrenova, Yu. G. Shvedenkov, A. V. Virovets, L. A. Sheludyakova and S. V. Larionov, *Russ. J. Inorg. Chem.*, 2007, **52**, 46-51; (b) Y. M. Klein, N. F. Sciortino, C. E. Housecroft, C. J. Kepert, and S. M. Neville, *Magnetochemistry*, 2016, 2-8.

2. (a) O. G. Shakirova, L. G. Lavrenova, Y. G. Shvedenkov, G. A. Berezovskii, D. Y. Naumanov, L. A. Sheludyakova, G. V. Dolgushin and S. V. Larionov, *Russ. J. Coord. Chem.,* 2004, *30*, 473-479; (b) M. Thomann, O. Kahn, J. Guilhem and F. Varret, *Inorg. Chem.,* 1994, **33**, 6029-6037.

3. (a) H. Z. Scott, T. M. Ross, B. Moubaraki, K. S. Murray and S. M. Neville, *Eur. J. Inorg. Chem.,* 2013, 803-812; (b) Y. Garcia, P. Guionneau, G. Bravic, D. Chasseau, J. A. K. Howard, O. Kahn, V. Ksenofontov, S. Reiman and P. Gütlich, *Eur. J. Inorg. Chem.,* 2000, 1531-1538; (c) G. Vos, R. A. Le Febre, R. A. G. de Graaff, J. G. Haasnoot and J. Reedijk, *J. Am. Chem. Soc.,* 1983, **105**, 1682-1683; (d) J. J. A. Kolnaar, G. van Dijk, H. Koojiman, A. L. Spek, V. Ksenofontov, P. Gütlich, J. G. Haasnoot and J. Reedijk, *Inorg. Chem.,* 1997, **36**, 2433-2440; (e) D. Savard, C. Cook, G. D. Enright, I. Korobkov, T. J. Burchell and M. Murugesu, *CrystEngComm.,* 2011, **13**, 5190-5197.

4. (a) V. Gómez, J. Benet-Buchholz, E. Martin and J. R. Galan-Máscarós, *Chem. Eur. J.* 2014, **20**, 5369-5379; (b) V. Gómez, C. S. de Pipaón, P. Maldonado-Illescas, J. C. Waerenborgh, E. Martin, J. Benet-Buchholz and J. R. Galan-Máscarós, *J. Am. Chem. Soc.*, 2015, **137**, 11924-11927.

5. N. Pittala, F. Thétiot, S. Triki, K. Boukheddaden, G. Chastanet, and M. Marchivie*, Chem. Mater.*, 2017, **29***,* 490-494.

6. H. O. Bayer, R. S. Cook and W. C. Von Mayer, *US Patent*, 1974, 3821376.

7. (a) S. Lethu and J. Dubois, *Eur. J. Org. Chem.,* 2011, 3920-3931; (b) P. G. Baraldi, F. Fruttarolo, M. A.Tabrizi, D. Preti, R. Romagnoli, H. El-Kashef, A. Moorman, K. Varani, S. Stefania Gessi, S. Merighi and P.A. Borea, *J. Med. Chem.,* 2003, **46***,* 1229-1241; (c) G. Dupouy, M. Marchivie, S. Triki, J. Sala-Pala, J.-Y. Salaün, C. J. Gómez-García and P. Guionneau, *Inorg. Chem.*, 2008, **47**, 8921-8931.

8. G. M. Sheldrick, *Acta Cryst*., 2008, **A64**, 112-122.